The Astrophysical Journal, 694:1471–1480, 2009 April 1 doi:10.1088/0004-637X/694/2/1471

THE STRUCTURE OF STREAMER BLOBS

N. R. Sheeley, Jr., D. D.-H. Lee[1], K. P. Casto[2], Y.-M. Wang, and N. B. Rich[3]
Space Science Division, Naval Research Laboratory, Washington, DC 20375-5352, USA; sheeley@spruce.nrl.navy.mil
Received 2008 November 26; accepted 2009 January 8; published 2009 March 24

ABSTRACT

We have used Sun–Earth Connection Coronal and Heliospheric Investigation observations obtained from the *STEREO* A and B spacecraft to study complementary face-on and edge-on views of coronal streamers. The face-on views are analogous to what one might see looking down on a flat equatorial streamer belt at sunspot minimum, and show streamer blobs as diffuse arches gradually expanding outward from the Sun. With the passage of time, the legs of the arches fade, and the ejections appear as a series of azimuthal structures like ripples on a pond. The arched topology is similar to that obtained in face-on views of streamer disconnection events (including in/out pairs and streamer blowout mass ejections), and suggests that streamer blobs have the helical structure of magnetic flux ropes.

Key words: Sun: corona – Sun: coronal mass ejections (CMEs) – Sun: magnetic fields

1. INTRODUCTION

In 1996–1997, observations with the Large Angle Spectrometric Coronagraph (LASCO) on the *Solar and Heliospheric Observatory* (*SOHO*) spacecraft revealed a continuous flow of density inhomogeneities moving radially outward along coronal streamers, apparently tracing the flow of the slow solar wind (Sheeley et al. 1997). The inhomogeneities originated about 3–4 $R_\odot$ from Sun center as small blobs of material, about 1 $R_\odot$ in length and 0.1 $R_\odot$ in width, detaching from the cusps of coronal streamers. As they moved outward, their lengths increased in rough proportion to their speeds, which typically doubled from 150 km s^{-1} near 5 $R_\odot$ to 300 km s^{-1} near 25 $R_\odot$, corresponding to an acceleration of about 4 m s^{-2}. Height/time maps revealed these motions as a series of tracks, occurring at the rate of about four per day (Wang et al. 1998; Sheeley 1999; Sheeley et al. 1999). Wang et al. (1998) suggested that these streamer blobs are injected into the solar wind as a result of footpoint exchanges between the stretched loops of streamer magnetic field and the neighboring open magnetic field lines. Crooker et al. (2004) have identified localized polarity reversals in the heliospheric plasma sheet, which may be the in situ signatures of streamer blobs in the solar wind.

The intensities of the blobs were ∼10% of the intensities of their associated coronal streamers. Consequently, these faint features were most easily seen in running difference images, which often showed forked or chevron-shaped structures with prongs extending radially outward along the sides of the ejections (Wang et al. 1998). When these structures were visible in unsubtracted images, they appeared with circular or concave-outward shapes similar to those observed for streamer detachments (Wang et al. 1999; Wang & Sheeley 2006) and flux-rope coronal mass ejections (CMEs; Thernisien et al. 2006). Such streamer eruptions seemed to originate when the loops of an expanding magnetic arcade reconnected with each other to form an outgoing helical arch and a collapsing loop system, as illustrated in Figure 3(a) of the paper by Gosling et al. (1995). When the streamer is seen face-on, the outgoing component appears as a giant arch or slinky, and when the streamer is seen edge-on, the outgoing component appears as a two-pronged fork. Thus, it seemed plausible that streamer blobs might also have this flux-rope topology.

Now, coronal observations from the *Solar Terrestrial Relations Observatory* (*STEREO*) twin spacecraft, A and B, are providing complementary observations of these streamer-related events. These two spacecraft are in near-Earth orbits, with A slightly closer to the Sun and drifting ahead of the Earth and B slightly farther from the Sun and falling behind. They are separating at the rate of approximately 45° per year and were 56° apart in 2008 June when some of these observations were taken. Their separation will be 90° on 2009 January 24.

Each spacecraft is equipped with a suite of Sun–Earth Connection Coronal and Heliospheric Investigation (SECCHI) instruments (Howard et al. 2008). In addition to an extreme-ultraviolet imager (EUVI), there are two coronagraphs (COR1 and COR2), and two off-pointed heliospheric imagers (HI1 and HI2). COR1 and COR2 are centered on the Sun and have annular fields of view (FOVs) of 1.3–4.0 $R_\odot$ and 2–15 $R_\odot$, respectively. HI1 is pointed 13.°2 away from the Sun and shows a 20° field centered near the ecliptic. HI2 is pointed about 53.°4 from the Sun and shows a 70° field also centered near the ecliptic. The HI1 and HI2 telescopes on the A spacecraft are pointed east of the Sun, and the corresponding telescopes on the B spacecraft are pointed west of the Sun. Thus, each suite of telescopes spans an FOV whose dimensions extend outward to 88.°4 from the Sun in the east or west direction, but to a projected distance of only 15 $R_\odot$ over the Sun's poles.

Whereas the streamer belt lay close to the equator during 1996–1997, it has extended to higher latitudes during 2007–2008, apparently as a consequence of the weaker polar field during the present sunspot minimum era (Sheeley 2008). The result has been a stable streamer pattern with poleward excursions around the long-lived, low-latitude coronal holes. Together, these poleward excursions and the increased longitudinal separation of the *STEREO* spacecraft are providing an opportunity to obtain simultaneous edge-on and face-on views of the streamer belt under conditions of low sunspot activity. As we shall see next, these complementary views are revealing the three-dimensional helical structure of streamer blobs.

[1] Now at Carnegie-Mellon University, Pittsburgh, PA 15213, USA.
[2] Now at Thomas Jefferson High School of Science and Technology, Alexandria, VA 22312, USA.
[3] Interferometrics, Inc., Herndon, VA 20171, USA.

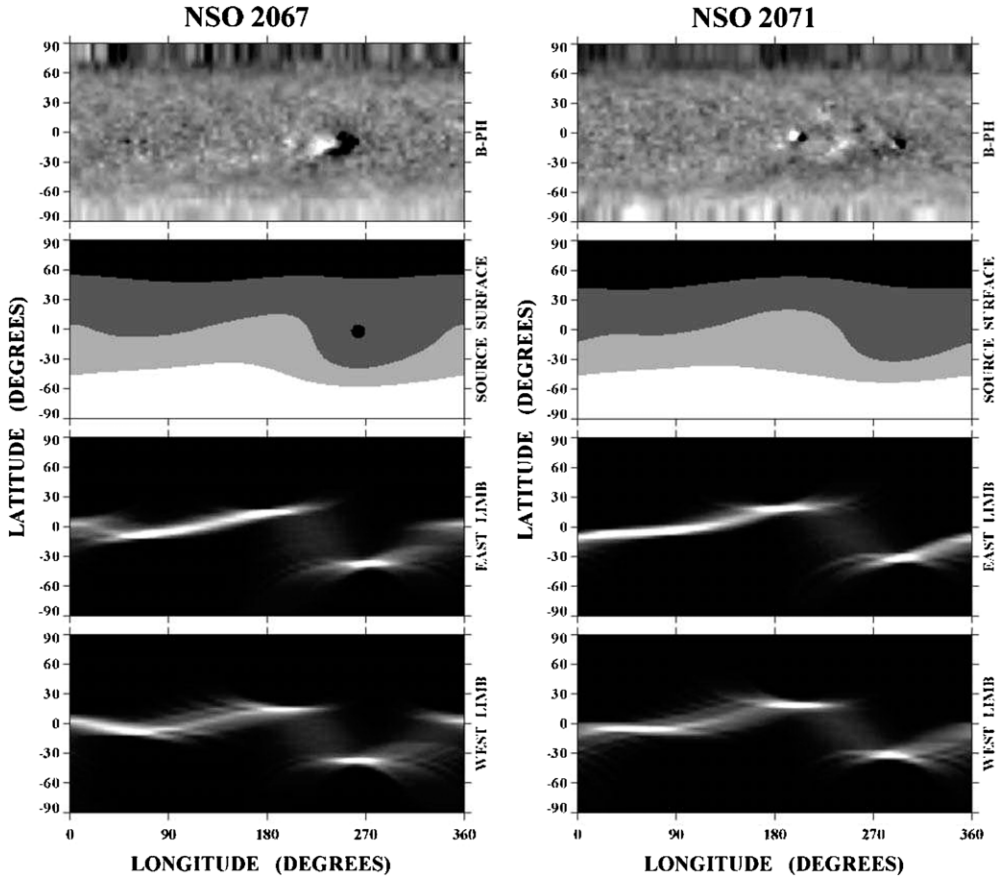

Figure 1. Carrington maps of the National Solar Observatory (NSO) observed photospheric field (top), the derived source-surface field at 2.5 $R_{\odot}$, and the simulated east-limb and west-limb coronal intensity at 3.0 $R_{\odot}$ during rotations 2067 (2008 February 21–March 20) and 2071 (2008 June 9–July 7), showing the warped pattern associated with the active longitude near 270°. At this longitude, the streamer belt is deflected almost to S30°.

2. OBSERVATIONS

Figure 1 compares Carrington maps of photospheric field and its source-surface extension derived from Synoptic Optical Long-term Investigations of the Sun (SOLIS) measurements at Kitt Peak during rotations 2067 (2008 February 21–March 20) and 2071 (2008 June 9–July 7). Simulations of the east-limb and west-limb coronal intensity at 3.0 $R_{\odot}$, derived using the method of Wang et al. (1997), are shown in the bottom panels. Despite the relatively low level of solar magnetic activity, the source-surface neutral line and associated streamer belt have a wavy appearance whose extremes extend to about 30° latitude. This is unusual at sunspot minimum when the streamer belt is normally confined to a narrow region at the equator, as it was 11 years ago in 1997. The unusually large latitudinal extent of the streamer belt during the present sunspot minimum era is due to the relatively weak polar magnetic field combined with the occurrence of sunspot activity in an active longitude near 270°. As discussed by Wang et al. (1997), by erupting in longitudinal phase, even a relatively small amount of flux can oppose the background field (especially when it is unusually weak) and deflect the streamer belt away from the equator.

Figure 2 shows two views of the corona on 2008 June 19, one from the COR2-B white-light coronagraph (top) and the other from the COR2-A coronagraph (bottom), when the A spacecraft was located about 56° west of the B spacecraft. Each image is displayed with solar north at the top and east to the left. The image from B shows a predominantly edge-on streamer in the southwest quadrant. We have marked its boundaries by two black lines. The image from A shows the same streamer as it looks from above, again bounded by two black lines. This is the face-on view that one obtains from a Carrington longitude slightly greater than 270° and shows the southernmost extremity of the streamer belt. If the streamer belt had been confined to the equator as it was 11 years ago in 1997, the *STEREO* spacecraft would not have obtained such a view from above until the sunspot cycle progressed to a more active phase.

Figure 3 shows a sequence of running difference images during the interval 2136 UT June 18–0649 UT June 20. (The running difference images have not been rolled to make solar north directly up and small corrections less than 8° are indicated in the respective captions of this paper.) Whereas a blob (indicated by the arrows) was hardly visible in the unsubtracted images in Figure 2, it is clearly visible as a leading-white/trailing-black density enhancement moving through the panels of Figure 3. In the upper-left panel at 2136 UT, the COR1-B image shows the trailing edge of the blob as it was pulling away from the top of the helmet. The next panel at 2138 UT shows this blob entering the COR2-B FOV behind a fainter blob near the center of the field. As the intense blob moved through the COR2-B FOV, its edges projected forward ahead of its center to produce a concave-outward shape. This shape is still visible in the lower-right panel, which shows the blob a day later leading a sequence of blobs outward through the HI1-B FOV.

Figure 4 shows a corresponding sequence of COR2-A running difference images during June 18–19. Whereas our view from the B spacecraft showed a diffuse blob evolving into a forked

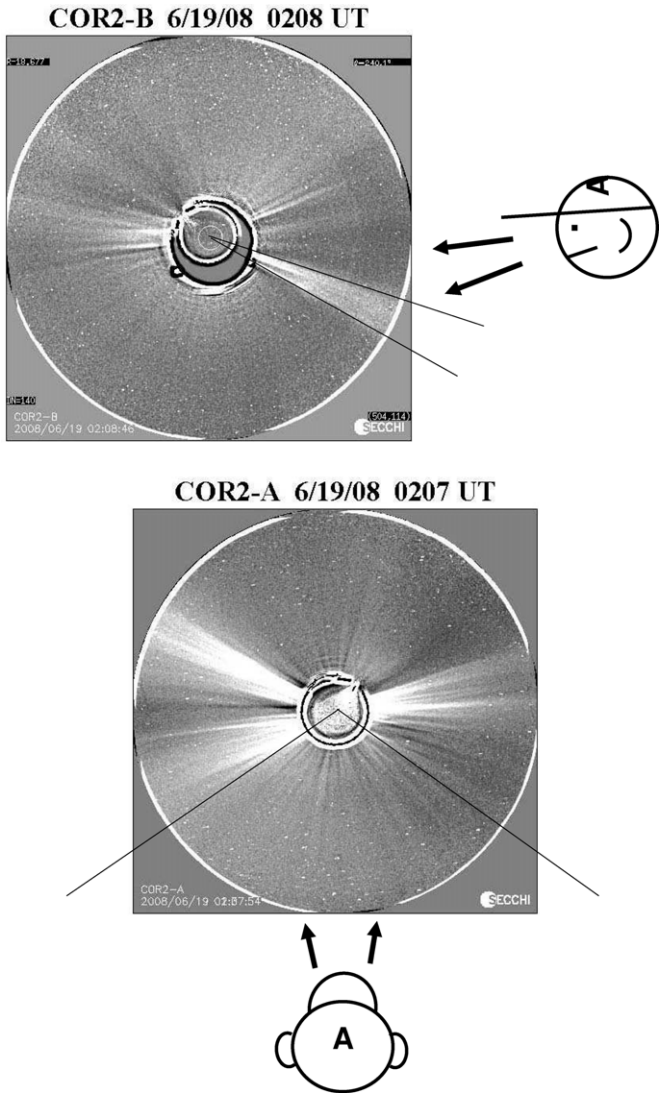

Figure 2. Near simultaneous images of the white-light corona between ~2 $R_\odot$ and 15 $R_\odot$, obtained from the COR2-B (top) and COR2-A (bottom) instruments on 2008 June 19, showing nearly edge-on and face-on views of the southward-deflected portion of the streamer belt. The cartoon character represents the A spacecraft looking down on this segment of the streamer. These images have been rotated slightly to place solar north upward.

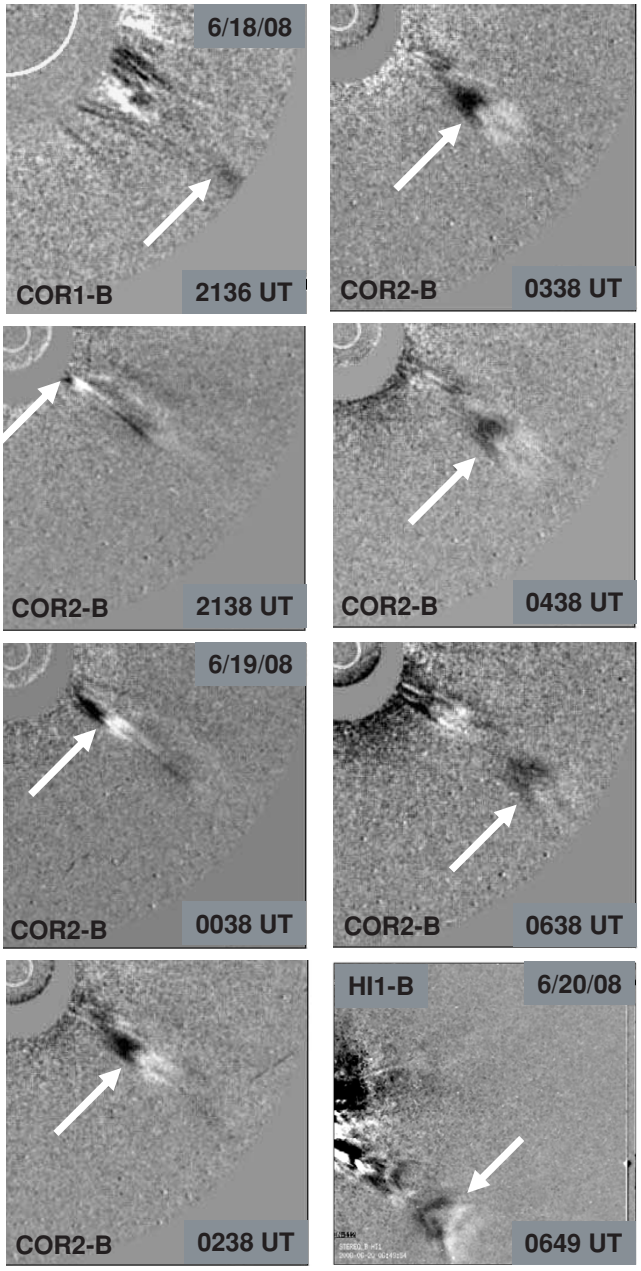

Figure 3. Time sequence of running difference images obtained from the B spacecraft during June 18–20, showing the outward motion of a "forked blob" (white arrows) along the edge-on projection of the streamer. We have not rotated the running difference images of this paper, and solar north is 7.°4 clockwise from the top.

structure, our view from A shows a large arch, spanning a wide range of position angles in the southeast quadrant. Its legs fade with time, eventually leaving a predominantly azimuthal structure moving through the FOV with the characteristic leading-white/trailing-black signature of an intensity enhancement.

Although we have no doubt that Figures 3 and 4 show two views of the same ejection, we think it is instructive to consider the detailed geometry that relates these two views. For this purpose, we suppose that the ejection is directed along a radius vector extending from the center of the Sun outward into the heliosphere. A position angle, pa, determines the azimuth of this radius vector around the observer–Sun line, and an inclination angle, δ, determines how far the radius vector is elevated above (or below) the sky plane. As we shall see later, these two angles are convenient for analyzing elongation/time tracks of solar ejections.

Here, our problem is to relate the coordinates in one view, say from the B spacecraft, to the coordinates in the other view from the A spacecraft. As described elsewhere (N. R. Sheeley et al. 2009, in preparation), we link these coordinates through the Carrington coordinates of their projections back at the Sun. In particular, we find the footpoint of the radius vector seen from the B spacecraft and express its heliographic co-latitude, θ_B, and longitude, ϕ_B, in terms of the coordinates (pa_B, δ_B). Similarly, we find the footpoint of that same radius vector seen from the A spacecraft and express its heliographic coordinates, (θ_A, ϕ_A), in terms of (pa_A, δ_A). Then, because the values of co-latitude are the same for both spacecraft and the values of longitude differ by a known value (comparable to the angular ecliptic separation between A and B), we obtain two equations relating (pa_B, δ_B) and (pa_A, δ_A).

We have used these relations to generate the plots in Figure 5. Here, we recognize that in the edge-on view, the blob's position

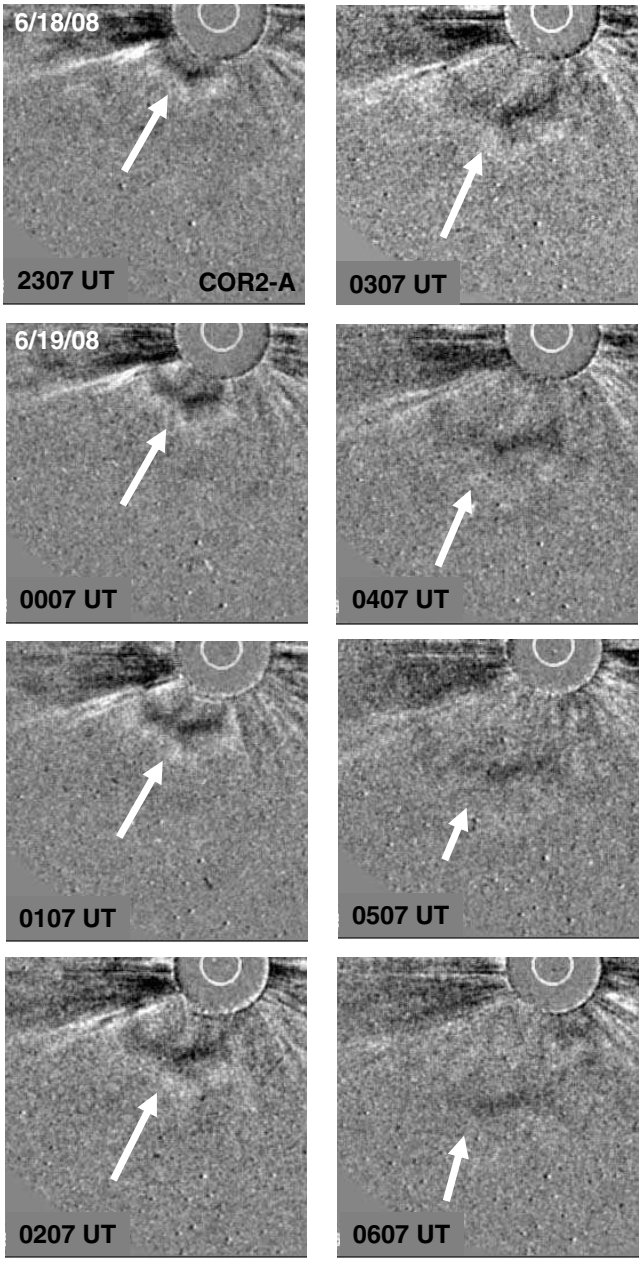

Figure 4. Time sequence of running difference images obtained from the A spacecraft during June 18–19, showing that the forked blob in Figure 3 appears as an expanding arch when viewed from above. Here, solar north is 6.0 clockwise from the top.

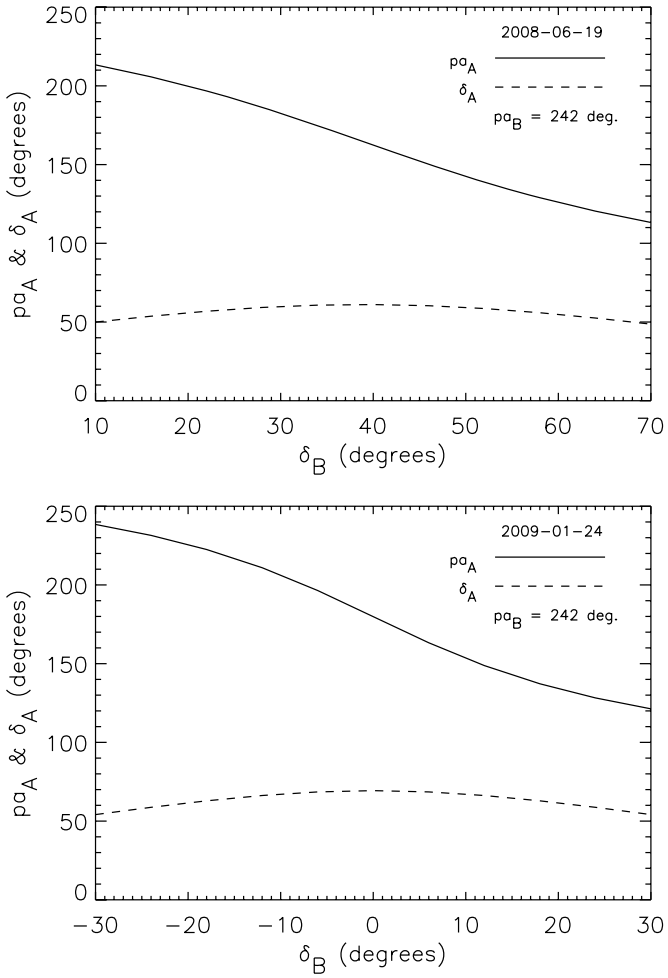

Figure 5. Top: plots of a blob's position angle, pa_A, and sky-plane elevation angle, δ_A, seen from the A spacecraft as a function of its elevation, δ_B, as seen from the B spacecraft on 2008 June 19 when the spacecraft separation was 56°. Bottom: similar plots for 2009 January 24 when the spacecraft separation will be 90°. We set $pa_B = 242°$ in each case. As expected, δ_A is confined to a narrow range of values near 55°, while pa_A spans a wide range of values corresponding to the approximate width of the arch.

angle, pa_B, has a well-defined value ∼240°, but that its elevation angle, δ_B, out of the sky plane may extend through a wide range of values. Consequently, in the top panel, we select the observed value of $pa_B = 242°$ for 2008 June 19, and plot pa_A and δ_A as a function of δ_B. For values of δ_B in the range 10°–70°, we obtain values of pa_A (solid curve) in the range 110°–210°, roughly corresponding to the angular span of the arch seen in the face-on views in Figure 4. The value of δ_A (dashed curve) is confined to a narrower range of 50°–60°, corresponding to the approximate co-latitude of the streamer seen in the edge-on views of Figures 2 and 3. The negative slope of the solid curve indicates that the leg of the arch that is closer to the observer in the edge-on view lies closer to the equator in the face-on view.

We might wonder why the dashed curve attains its maximum value when $\delta_B \approx 40°$ rather than when $\delta_B = 0°$, which one would expect for an edge-on view. The answer is that on 2008 June 19, the A and B spacecraft are separated by 56°, not 90° as suggested by the cartoon character in Figure 2. As shown in the bottom panel, the dashed curve does attain its maximum value at $\delta_B = 0°$ on 2009 January 24 when the separation will be 90°. Although the cartoon character provides a convenient way of understanding the stereoscopic geometry, those complementary views will not be fully orthogonal until January 24.

As mentioned in the introduction of this paper, streamers emit blobs repeatedly at a rate of about four per day (Wang et al. 1998; Sheeley 1999). Consequently, in the face-on views, we would expect the arches to occur in a continuous sequence, like surface waves moving out from a distant source. In Figure 6, we show a sequence of blobs, numbered consecutively 1–3, whose face-on views do show a series of azimuthal structures on June 18–19. Blob 2 is the bright feature shown in Figures 3 and 4, and blob 1 is the fainter blob that preceded it. In the face-on views, these azimuthal structures fade quickly as they move out through the field and are replaced by the next one in the sequence.

Figure 7 shows elongation/time maps of these motions along slits placed at position angles of 240° and 150°. These maps were constructed using Adam Herbst's modification

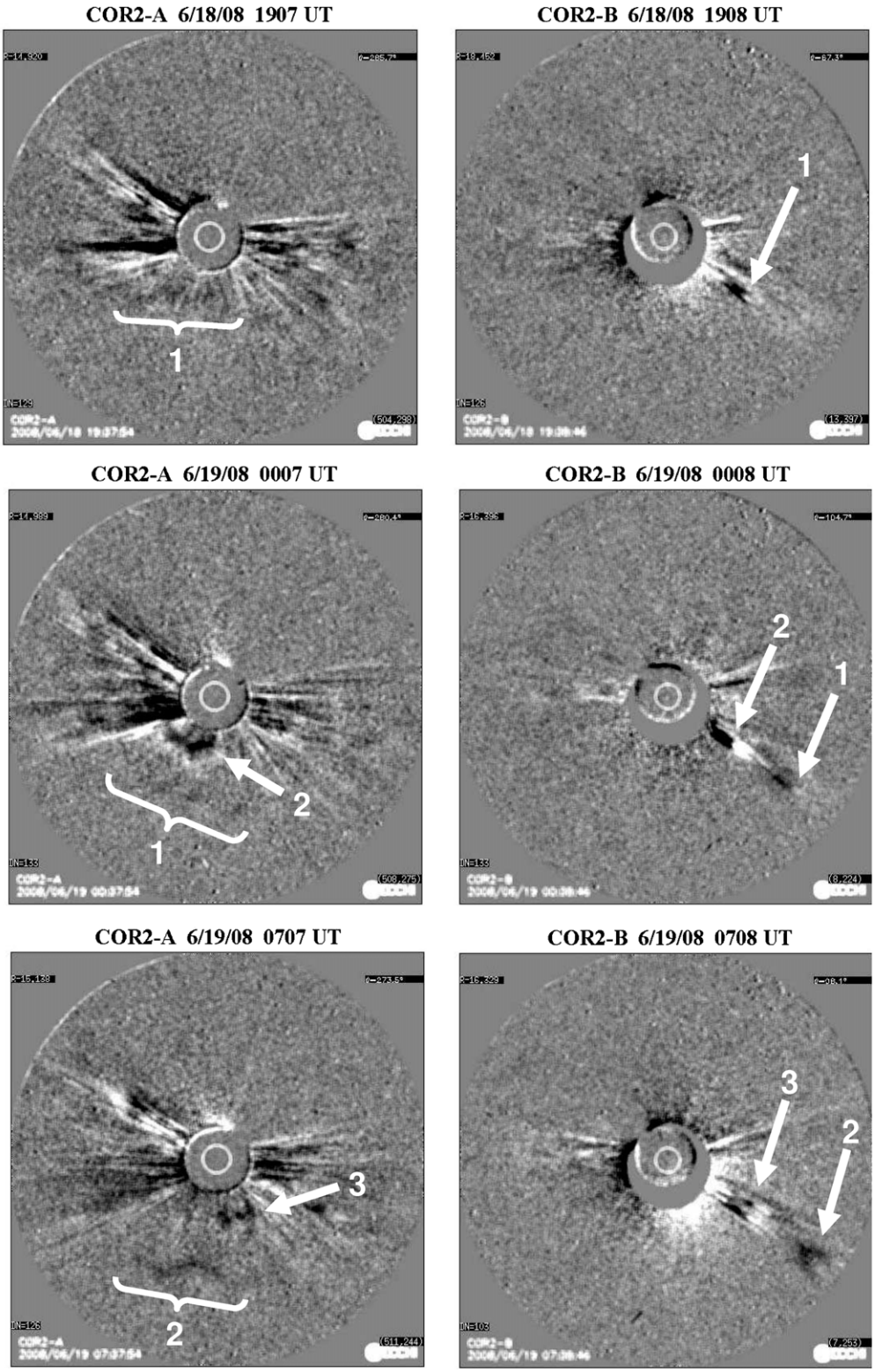

Figure 6. Sequences of COR2-A images (left) and COR2-B images (right) while the three blobs move across the FOVs. The series of blobs in the edge-on views appears as a series of azimuthal waves in the face-on views.

of the technique developed by Jeffery Walters for LASCO coronagraph observations (Sheeley et al. 1999, 2008a, 2008b). In Walters' procedure, radial strips are cut from a sequence of running difference images and placed chronologically to form a rectangular map of intensity difference as a function of time (on the horizontal axis) and projected radial distance (on the vertical axis). In Herbst's extension to the SECCHI data, the off-pointed and wide-field HI1 and HI2 images are transformed to a Sun-centered polar coordinate system whose radial coordinate is elongation angle and whose azimuthal coordinate is solar position angle, before the radial strips are extracted. Consequently, the vertical axis becomes solar

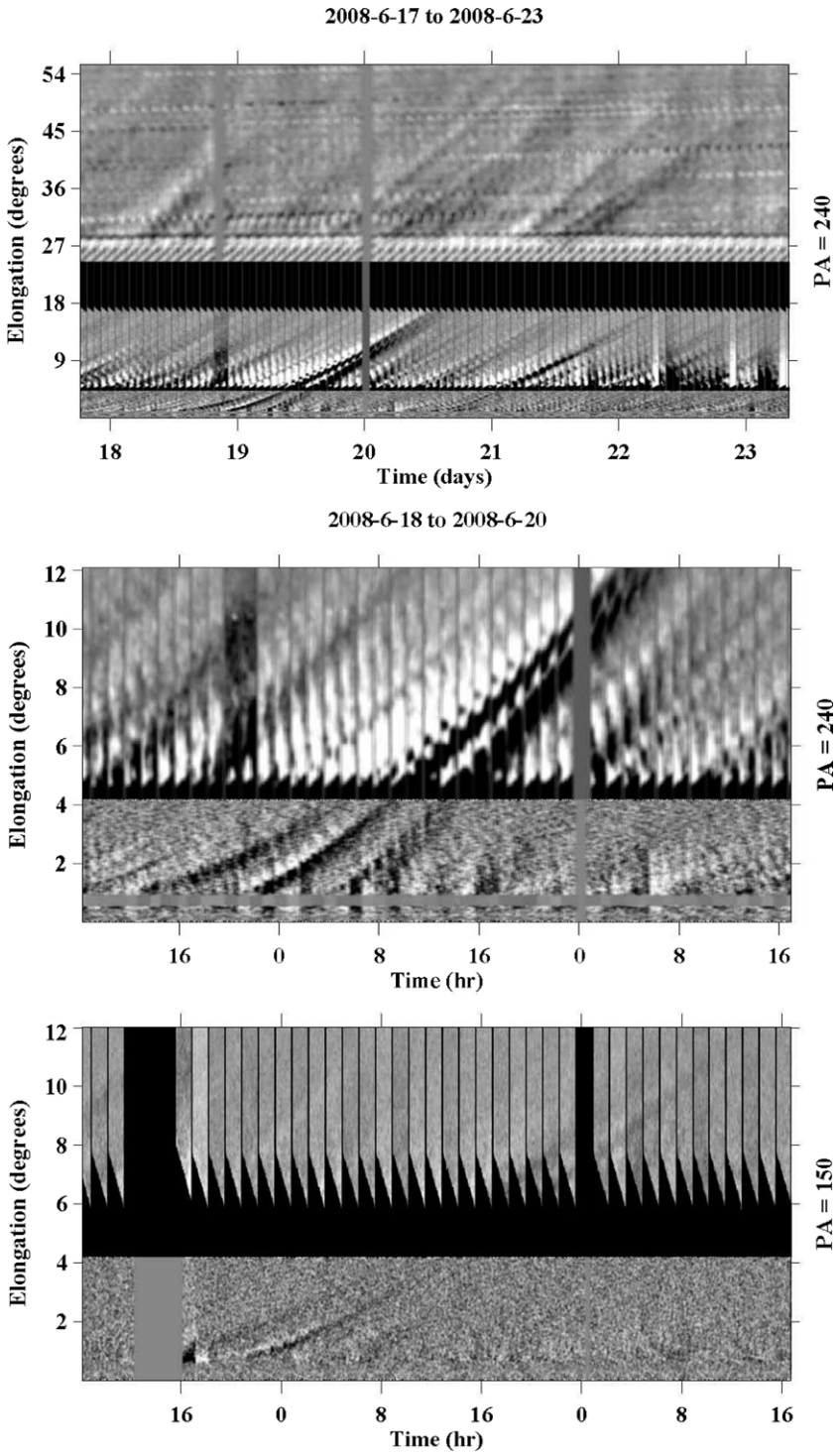

Figure 7. Elongation/time maps showing tracks of the three blobs in Figure 6. The tracks in the upper panel were obtained at a position angle of 240° and can be traced across the fields of COR2-B, HI1-B, and HI2-B. The lower panels compare the tracks at 240° with those obtained from the A spacecraft at 150°. At such high latitudes, there are dark data gaps between the COR2 and HI1 observations.

elongation angle, and the map shows tracks of elongation angle versus time.

The upper panel of Figure 7 shows an elongation/time map constructed from running difference images obtained by the COR2-B, HI1-B, and HI2-B instruments during the interval 2008 June 17–23. Because the streamer projected southward at a position angle of approximately 240°, and the HI1 and HI2 images are centered at the equator, a dark gap occurs in the elongation range 17°–25° between the two FOVs. This makes it difficult to associate the tracks below 17° with those above 25°, and therefore difficult to determine the radial speed, v_r, and elevation angle, δ_B, of the ejection using the curve-fitting technique described previously (Sheeley et al. 2008a; Rouillard et al. 2008). However, the COR2-B/HI1-B track of the central blob seems to line up best with the second of the three tracks in HI2-B. If we use this extension, then we obtain $v_r \sim 350$ km s^{-1} and $\delta_B \sim 30°$, which are consistent with the values that one would expect for a blob seen edge-on near the sky plane.

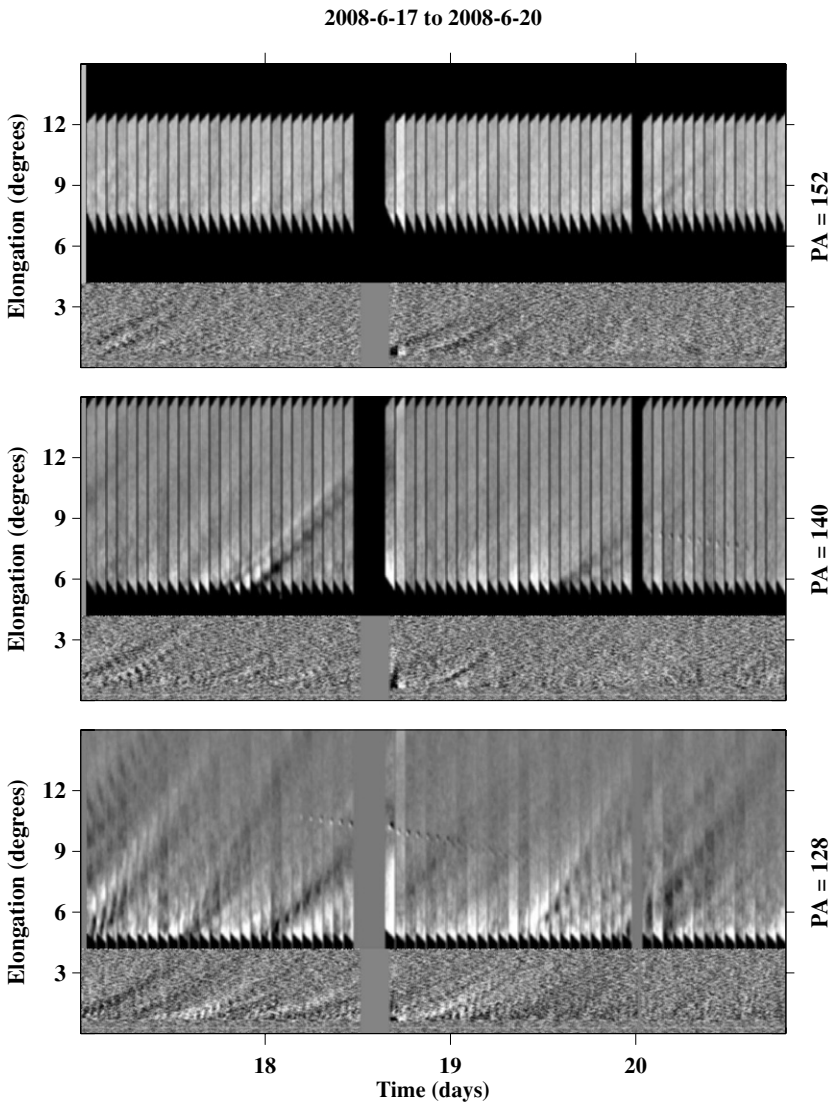

Figure 8. Elongation/time maps obtained for a range of position angles seen by the A spacecraft on 2008 June 17–20, showing the different character of the tracks when blobs are seen face-on (top and middle panels) and edge-on (bottom panel).

We can then find the coordinates as seen from the A spacecraft using the plots in the top panel of Figure 5: $pa_A \sim 180^\circ$ and $\delta_A \sim 60^\circ$. This suggests that we are tracking the southernmost end of the arch.

The HI1-A and HI2-A FOVs do not extend this far from the equator. Nevertheless, we were able to make an elongation/time map at a position angle of 150° and compare it with an enlarged and cropped version of the map at 240° in the bottom two panels of Figure 7. The tracks of the three blobs seen clearly with the B spacecraft are faintly visible in the elongation/time map obtained at 150° with the A spacecraft. As expected for motions so far out of the sky plane, the tracks at 150° have smaller slopes than those in the more edge-on view at a position angle of 240°, and reach the 12° limit of these panels about 8 hr after the tracks at 240°.

Although 150° is near the upper limit of position angles that are suitable for making elongation/time maps with the combined COR2/HI1-A observations, we can make these maps at smaller position angles to see how the tracks vary with position along the arch. Figure 8 compares COR2/HI1-A maps at position angles of 152°, 140°, and 128° during the four day interval June 17–20. Although the map at 152° shows a large data gap between the COR2 and HI1 fields (and above the HI1 field as well), it shows tracks of the three blobs during June 18–19 as well as tracks of similar blobs seen face-on during June 17–18. The map at 140° shows some of these tracks with smaller data gaps. The map at 128° lies closest to the equator where gaps are no longer a problem. However, it also encounters a streamer seen edge-on from the A spacecraft (see Figures 2 and 4), and shows a different set of elongation/time tracks. As we have seen in Figure 7, the blobs occur more frequently in the edge-on views than they do in the face-on views. Because the blobs are confined to a narrow sheet, they appear brighter and more numerous when the line of sight lies in the sheet than when it is directed perpendicular to the sheet. Also, the elongation/time tracks have greater maximum slopes in the edge-on views where most of the ejections are directed close to the sky plane, than in the face-on views where the ejections lie farther out of the sky plane. The greater slopes obtained in the edge-on views will be closer to the true radial speeds (300–400 km s^{-1}) of the blobs.

The June sequence of arched-shaped blobs was not an isolated occurrence. We have observed similar sequences on 2008 April 25–26, September 7–8, and October 4–5 at approximately this

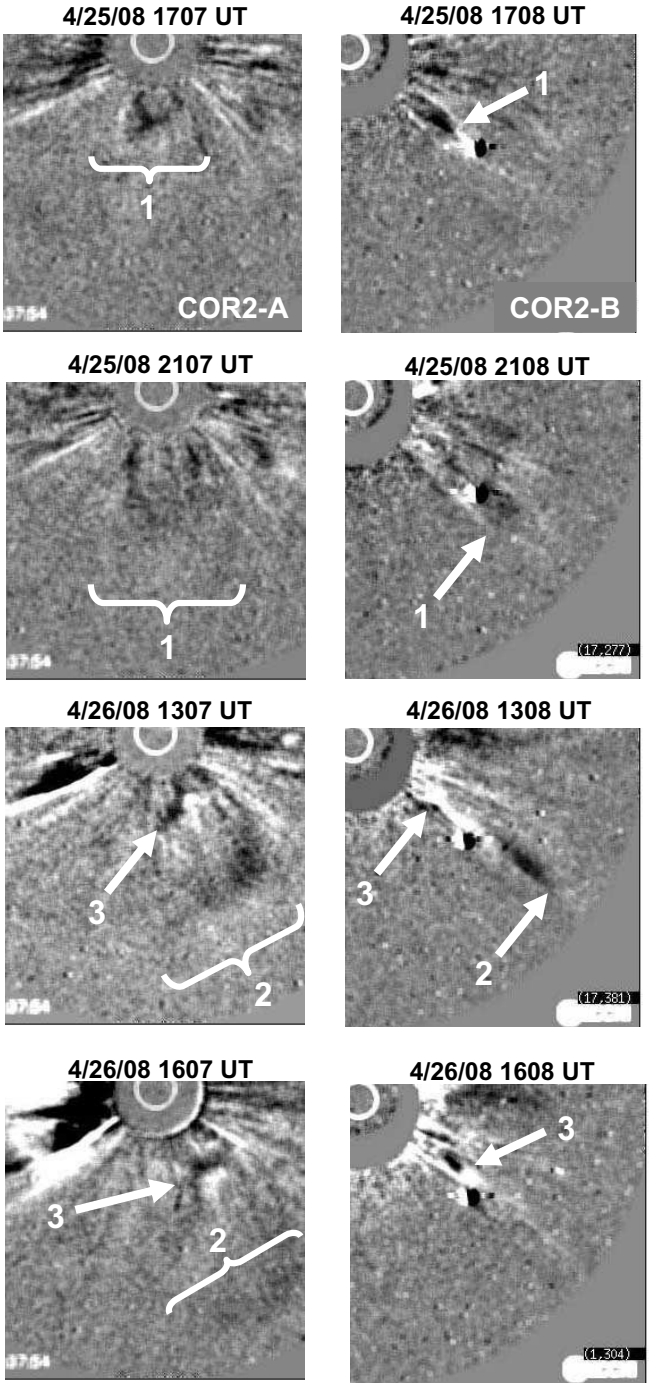

Figure 9. Sequences of COR2-A (left) and COR2-B (right) images, comparing a sequence of streamer blobs (labeled 1, 2, and 3) in face-on and nearly edge-on views during 2008 April 25–26. The intense black/white feature near the center of the COR2-B images is Venus. Solar north is 7°.6 clockwise from the top in the A images and 3°.4 clockwise in the B images.

same Carrington longitude. Figure 9 shows part of the April sequence and Figure 10 compares blob 2 on June 19 with a similar arch-shaped blob on October 4 when the streamer lay closer to the equator.

Figure 11 compares edge-on and face-on views of a somewhat larger streamer disconnection event (indicated by the white arrows) at this 270° Carrington longitude on 2008 May 23–24. The upper-right panel shows the pinchoff as it occurred in the COR1-B running difference image at 1956 UT on 2008 May 23. In the upper-left panel, the ejection consists of a large arch. By 0038 UT on May 24, the COR2-B image shows the familiar concave-outward shape of the ejection, and the COR2-A image shows some fine structure at the lower edge of the expanding arch. (Intense features, coming in from the southwest in COR1-A and from the southeast in COR1-B, indicate a sungrazing comet.)

3. SUMMARY AND DISCUSSION

We have made virtually simultaneous observations of streamer blobs when the *STEREO* A and B spacecraft obtained edge-on and face-on streamer views. The blobs have a concave-outward structure in the edge-on views and an arch topology in the face-on views. These configurations have been found previously in observations of streamer detachments, in/out pairs, and gradually accelerating CMEs (Wang & Sheeley 2006; Sheeley & Wang 2007), and are consistent with a magnetic flux-rope topology (Thernisien et al. 2006).

When viewed face-on, a series of streamer blobs appears as a series of arches that begin with both legs tied to the Sun. As the legs fade, the arches evolve into azimuthal waves. We suppose that the transition from a two-legged arch to an azimuthal wavefront is the consequence of being carried out passively in a uniform radial flow. This is the same kinematic effect that causes CMEs to evolve into "pancake" shapes as they move outward through the heliosphere (Riley & Crooker 2004). Consequently, in the face-on view of a streamer, we see azimuthal wavefronts moving toward us like water waves from a distant source. This is what we would expect the equatorial streamer belt to look like if we could observe it from above.

The expanding arches resemble the outward components of in/out pairs that we have observed with the LASCO coronagraphs (Sheeley & Wang 2002, 2007; Wang & Sheeley 2006). In/out pairs are density enhancements at the leading and trailing edges of depletions that occur when slowly rising coronal structures suddenly separate from the Sun. The outward component is shaped like a large arch with both ends attached to the Sun, and the inward component is often resolved into loops. We supposed that the separation occurs when the rising arcade of magnetic loops reconnects to produce an outgoing helical flux rope and an ingoing arcade of collapsing loops.

A puzzling aspect of the in/out pairs was their tendency to occur at high latitudes and occasionally to occur in a series of events over the Sun's poles. The observations of this paper suggest that these in/out pairs may have occurred at times that high-latitude segments of the streamer belt were located at the central meridian, providing face-on views from the *SOHO* spacecraft. Our preliminary examination of five intervals of repeating in/out pairs (7/29/03-N, 9/9/03-S, 11/9/03-N, 2/8/05-N, and 3/26/05-N) appears to confirm this idea.

An important question is whether all blobs have this flux-rope topology, or whether we are singling out a special subset consisting of the smallest events in a broad spectrum of streamer detachment events (Sheeley et al. 2007). During several Carrington rotations in 2008, sequences of bright blobs in the edge-on views were accompanied by the corresponding sequences of expanding arches in the face-on views. This supports the idea that all blobs have the flux-rope topology. During Carrington rotations 2072 (July 7–August 3) and 2073 (August 3–August 30), we found no obvious arches in the face-on views. However, at these times, the blobs were relatively faint in the edge-on views, so that arched counterparts, if they existed, may have been too faint to detect in the face-on views.

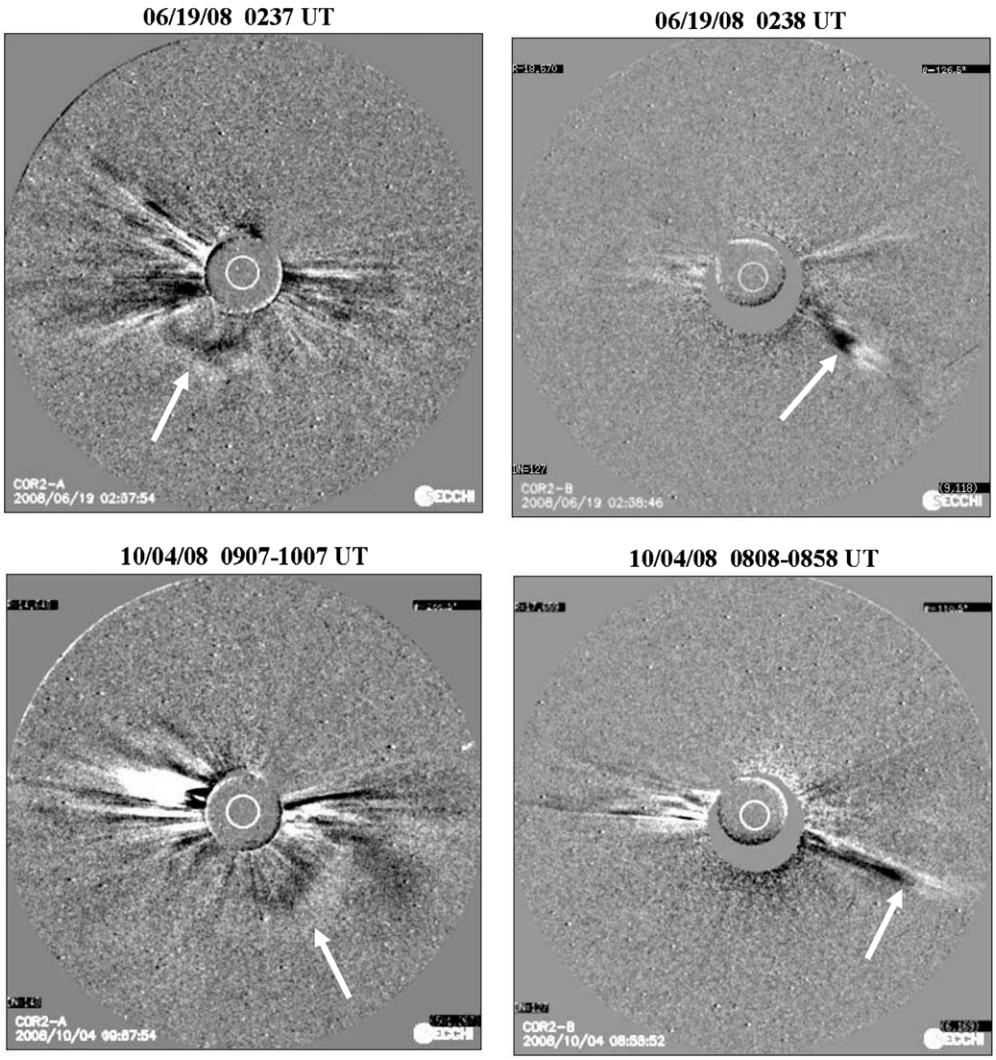

Figure 10. Comparison between complementary views of the 2008 June 19 blob (upper panels) and a blob on 2008 October 4 (lower panels) when the streamer lay closer to the equator. In each case, the blob appears as a large arch or azimuthal wave in the face-on view. Solar north is oriented 6.°0 clockwise (upper left), 7.°4 clockwise (upper right), 6.°2 counter clockwise (lower left), and 1.°2 clockwise (lower right).

If blobs are the small-scale part of a continuous spectrum of streamer eruptions, then we would expect the blobs and streamer eruptions to originate the same way. Observations of a streamer ejection during a particularly quiet interval in 2006 led us to the idea that the ejection had a nonmagnetic origin similar to the "leaky faucet" model that Hones (1979, 1985) proposed for the ejection of plasmoids in the Earth's magnetotail (Sheeley et al. 2007). In the leaky-faucet model, gravity opposes the surface tension of a slowly forming drop of water, causing the drop to elongate until it separates into an escaping component and a component that contracts back into the faucet. In our streamer model, a continuous source of material beneath the streamer would cause the streamer to inflate against the restraining tension of the magnetic field. Eventually, the plasma pressure would exceed the tension of the magnetic field, and the stretched loops would reconnect, releasing an outgoing flux rope and an arcade of collapsing loops. Thus, a coronal streamer would be like a leaky faucet, releasing flux ropes into the solar wind in an unending series of azimuthal waves.

Another question concerns the three-dimensional nature of the magnetic field line reconnection presumed to release the flux rope. Hughes & Sibeck (1987) added a "guide field" perpendicular to the noon–midnight meridian plane, and showed that in three dimensions the Hones' plasmoid becomes a flux rope. The flux rope remains tied to the Earth until it reconnects with open field lines along the flanks of the magnetotail. For a coronal streamer, we would expect the flux rope to remain connected to the Sun until it reconnects with open magnetic field lines outside the helmet. If one polarity was involved, a leg of the flux rope would be released, producing a coiled structure with only one end attached to the Sun. This is similar to the interchange reconnection previously envisioned (Wang et al. 1998), except that the newly opened field contains a coiled segment in the azimuthal direction. If two, oppositely directed, open field lines were involved, a portion of the flux rope would become disconnected from the Sun at both ends and escape into the solar wind as a coiled structure with both ends free. We would expect both kinds of reconnection to occur in the plasma sheet, slicing the flux rope into multiple segments and giving the wavefront its corrugated shape.

The *STEREO*/SECCHI data are produced by a consortium of the Naval Research Laboratory (NRL; US), the Lockheed Martin Solar and Astrophysics Laboratory (LMSAL; US), NASA/Goddard Space Flight Center (GSFC; US), the

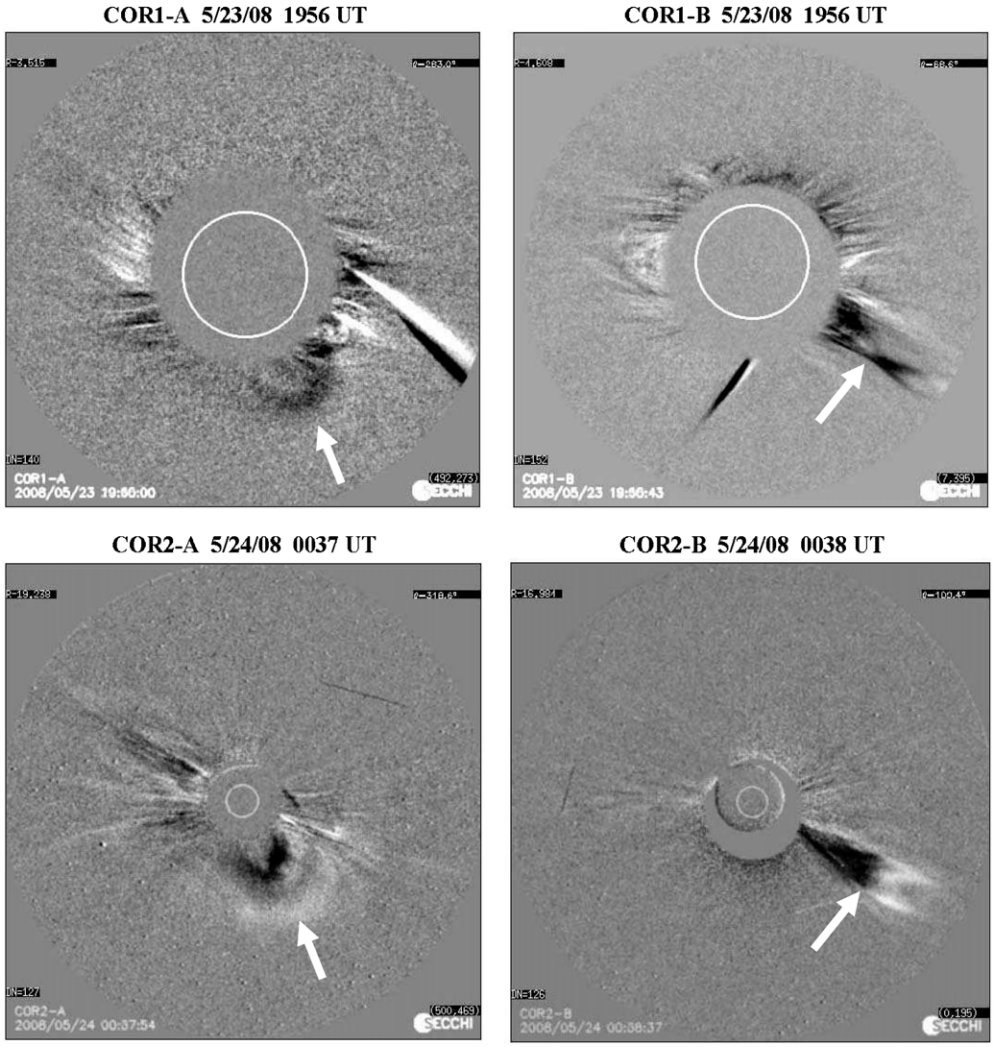

Figure 11. Near-simultaneous face-on and edge-on views of the same streamer on 2008 May 23–24 when a streamer detachment occurred. The face-on views from COR1-A and COR2-A show the characteristic arch structure, while the edge-on views from COR1-B and COR2-B show the pinchoff and concave-outward structure similar to that of a forked blob. Solar north is 7.°6 clockwise in the A images and 6.°1 clockwise in the B images. The bright streak coming in from the southwest in COR1-A and from the southeast in COR1-B is a sungrazing comet.

Rutherford Appleton Laboratory (RAL; UK), The University of Birmingham (UBHAM; UK), the Max Planck Institute for Solar System Research (MPS; Germany), CSL (Belgium), IOTA (France), and IAS (France). In the US, funding was provided by NASA, in the UK by Particle Physics and Astronomy Research Council (PPARC), in Germany by DLR, in Belgium by the Science Policy Office, and in France by CNES and CNRS. NRL received support from the USAF Space Test Program and ONR. We are grateful to our many colleagues in these organizations who made these observations possible. In particular, we acknowledge Lynn Simpson (Interferometrics, Inc.) for programming assistance in the display of COR1 and COR2 images and Karl Battams (NRL) for identifying planets and comets in the SECCHI images. The SOLIS data used in Figure 1 were produced cooperatively by NSF/NSO and NASA/LWS.

REFERENCES

Crooker, N. U., Huang, C.-L., Lamassa, S. M., Larson, D. E., Kahler, S. W., & Spence, H. E. 2004, J. Geophys. Res. (Space Phys.), 109, 3107
Gosling, J. T., Birn, J., & Hesse, M. 1995, Geophys. Res. Lett., 22, 869
Hones, E. W., Jr. 1979, Space Sci. Rev., 23, 393
Hones, E. W., Jr. 1985, Aust. J. Phys., 38, 981
Howard, R. A., et al. 2008, Space Sci. Rev., 136, 67
Hughes, W. J., & Sibeck, D. G. 1987, Geophys. Res. Lett., 14, 636
Riley, P., & Crooker, N. U. 2004, ApJ, 600, 1035
Rouillard, A. P., et al. 2008, Geophys. Res. Lett., 35, 10110
Sheeley, N. R. Jr. 1999, in AIP Conf. Ser. 471, Using LASCO Observations to Infer Solar Wind Speed Near the Sun, Proc. 9th Solar Wind Conf., Nantucket, MA, October 1998, ed. S. R. Habbal, R. Esser, J. V. Hollweg, & P. A. Isenberg (Melville, NY: AIP), 41
Sheeley, N. R., Jr. 2008, ApJ, 680, 1553
Sheeley, N. R., Walters, J. H., Wang, Y.-M., & Howard, R. A. 1999, J. Geophys. Res., 104, 24739
Sheeley, N. R., Jr., & Wang, Y.-M. 2002, ApJ, 579, 874
Sheeley, N. R., Jr., & Wang, Y.-M. 2007, ApJ, 655, 1142
Sheeley, N. R., Jr., Warren, H. P., & Wang, Y.-M. 2007, ApJ, 671, 926
Sheeley, N. R., Jr., et al. 1997, ApJ, 484, 472
Sheeley, N. R., Jr., et al. 2008a, ApJ, 675, 853
Sheeley, N. R., Jr., et al. 2008b, ApJ, 674, L109
Thernisien, A. F. R., Howard, R. A., & Vourlidas, A. 2006, ApJ, 652, 763
Wang, Y.-M., & Sheeley, N. R., Jr. 2006, ApJ, 650, 1172
Wang, Y.-M., Sheeley, N. R., Howard, R. A., Rich, N. B., & Lamy, P. L. 1999, Geophys. Res. Lett., 26, 1349
Wang, Y.-M., et al. 1997, ApJ, 485, 875
Wang, Y.-M., et al. 1998, ApJ, 498, L165